VOL. 18, NO. 12, JUNE 2023 ISSN 1819-6608
ARPN Journal of Engineering and Applied Sciences

www.arpnjournals.com

DEVELOPMENT OF A NOVEL TOOL USED TO SUPPORT DESIGN AND FAILURE ANALYSIS OF MULTIAXIAL FATIGUE LOADING: A CASE OF STEERING KNUCKLE

Aliyi Umer Ibrahim[1] and Dereje Engida Woldemichael[2]
[1]Department of Mechanical Engineering, School of Mechanical, Chemical and Material Engineering, Adama Science and Technology University, Adama, Ethiopia
[2]Department of Mechanical Engineering, College of Engineering, Addis Ababa Science and Technology University, Addis Ababa, Ethiopia
E-Mail: aliyiumer@yahoo.com

ABSTRACT

The steering knuckle requires a lot of attention when designing because once it is damaged it must be replaced with a new one. In automotive industry, since the structure of steering knuckles is very complex and different from each other; it is difficult to design it separately for each vehicle. In order to address this problem, an innovative idea to solve this problem was developed and named as analysis support tool for steering knuckle of the entire vehicle. In addition to that, the development of computer tool that can assist designers in the analysis phase can save the design time. For this purpose, analysis support tool for steering knuckles of entire vehicles has been developed. The part is first modeled by Free CAD 0.2 software considering the precision of the geometry. Based on scientific approach analysis support tool for steering knuckle of all vehicles is developed which can provide analysis of all forces acting on the component, maximum displacement, fatigue damage, maximum deflection, slope, factor of safety, life expectancy, stress and strain amplitude by stress and strain method and compare the results from Morrow, Smith Watson and Walker equations. In addition to that doing experiment of multiaxial is very expensive and time taking for the designer; therefore, developing simple, accurate and robustness tool used to determine life expectancy and cumulative fatigue damage of multiaxial which can be applied to entire materials is very crucial. The developed tool would be universal, effective, simple, and efficient method used to estimate the life expectancy and Cumulative fatigue damage of multiaxial. Finally, data's from open literatures are used to validate the accuracy and capabilities of the proposed tool for multiaxial fatigue loading. The end result is a computer tool that can be dedicated and run on any computer without using any internet connection.

Keywords: steering knuckle, multiaxial fatigue analysis, stress/ strain life, energy approach, factor of safety.

Manuscript Received 27 June 2023; Revised 19 August 2023; Published 30 August 2023

INTRODUCTION

The steering knuckle is an essential component of the vehicle suspension that houses the wheel hub or axle and connected to the suspension components. The wheel and tire assembly is attached to the knuckle's hub or spindle, which rotates the tire/wheel while keeping it in a balanced plane of motion by the knuckle/suspension system [1], [2], [3]. The wheel assembly is attached at its center to the steering knuckle. Note the protruding arm of the steering knuckle that attaches the steering mechanism to rotate it and wheel assembly. It is the connection between the steering knuckles, tie rod and axle beam by means of kingpins, which are attached to the suspension system as well. The wheel hub is fixed with the steering knuckle using bearings. The main function of it is to convert the linear movement of the tie rod into the angular movement [9], [10]. When the steering is turned by the driver, half part of the component subjected to a tensile load and half part of the component subjected to a compression load, and due to this wheel rotation, it is subjected to a torsional load [8], [6], [7]. Components of this part: A. Suspension Mounting Upper Strut Mount, B. Steering Arm, C. Lower Ball Joint D, Ball Bearing Location / Stub Hole, E. Brake Caliper Mounting and shown in Figure-1 below.

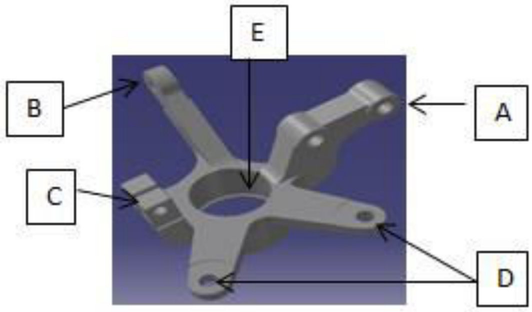

Figure-1. Components of Steering Knuckle by Free CAD 0.2 software.

Fatigue Analysis

Many structures that are used on daily basis exhibit multiaxial fatigue. It is necessary to assess the consequences of fatigue using modified models that take certain particular mechanisms into account. Engineers are frequently taken aback by the extensive list of criteria and are so many models to choose from. These models differ not just in the sorts of equations that they give, but also in the critical criteria that they use.

Recent technical demands for improving the performance of engineering components have highlighted the importance of proper component/system life. In today's

VOL. 18, NO. 12, JUNE 2023 ISSN 1819-6608
ARPN Journal of Engineering and Applied Sciences

technological demands, proper estimation of component life is required to escape sudden or unexpected failure. Steering knuckles are subjected to cyclic or alternating stresses [11-15], [32-33]. In addition to that, a complex variable stress is frequently caused by material flaws, geometric discontinuities (notches), etc. Thus, fatigue loading is the primary cause of failure for different parts (such as aeronautical engines and automotive transmission components) [6-7]. Therefore, in engineering applications, fatigue analysis taking into account complex load time history is crucial to guaranteeing mechanical structures [12], [18], [36-37]. To survive many cycles experience during its lifetime, fatigue analysis is the key points included in the analysis [19-27], [35], [38]. The methods used to predict the fatigue life include stress and strain life method. Only when stress & strain are present in the elastic region is the stress life approach is appropriate but the strain approach is appropriate for issues brought by plastic strain brought on by a concentration of stress [28-34], [39]. In its original form, the Smith Watson Topper (SWT) was created to calculate the fatigue life expectancy of materials for different a load-condition [37]. Table-3 shows the stress and strain amplitude equation used in the developed tool.

Multi-axial fatigue stresses are frequently applied to numerous hazardous structural components in engineering techniques, including engine turbine discs and blades. Additionally, mechanical structures' local stresses and strains at their bears, connections, and joints will exhibit a multi-axial stress state [42], [43], [44], [45], [46]. It is one of considerable technical significance to conduct multiaxial fatigue load analysis on important parts of engineering structures that are subjected to complex loads in order to more fully use the load-bearing capabilities of materials. When the structure's stress level is primarily in the elastic region, the stress-life approach performs well in estimating fatigue life. The detailed procedure of stress life method is shown in Figure-2 below.

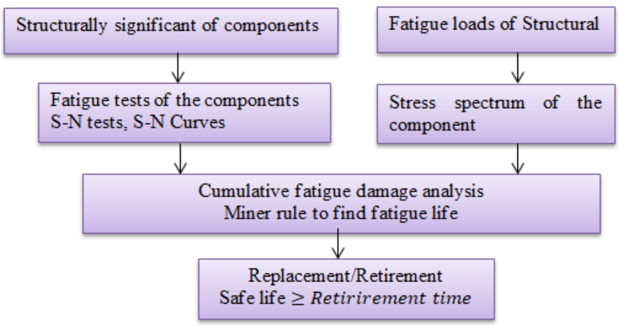

Figure-2. General Technique for calculating fatigue Safe-Life applying stress-life methods [47].

A multiaxial fatigue model based on strain was presented below for smooth and notched objects [48], [49].

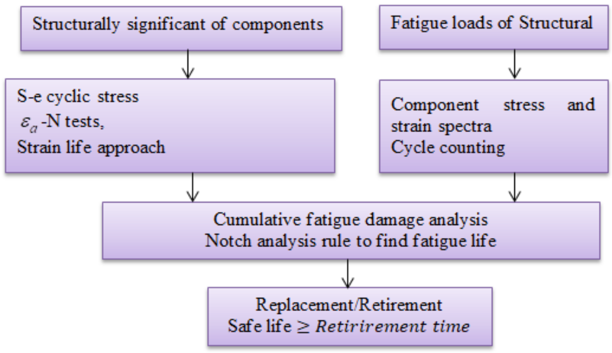

Figure-3. General Method for calculating the remaining and safe fatigue life using the strain-life approach [49].

The energy approaches not only have clear physical significance but also can escape the varied incremental plastic analysis, since energy comprises the interaction of the stress and strain [50], [51]. The energy criterion is suitable for the multiaxial fatigue loading failure mechanism; it cannot accurately depict the fatigue cumulative failure mechanism since the energy is a scalar [52]. Other researchers have also highlighted the drawbacks of the energy approach. First, the use of this criterion requires the use of an exact constitutive equation. Second, when the amount of plastic deformation is small, the plastic strain energy determination inaccuracy is undesired [53]. The strain energy density in the critical plane was believed to be more appropriate than stress or strain for fatigue life under uniaxial tension and compression [54], [55].

METHODOLOGY

A detail of the methodology is elaborated below. The corresponding flowchart is shown in Figure-4. The first stage includes preparation of revised design specification, detail design (i.e. force analysis acting on steering knuckle, maximum displacement, maximum deflection and slope), model it by using Free CAD 0.2 asper the design and procurement of standard part. Other key aspects of the design was multiaxial fatigue failure analysis by using Stress Life and Strain Life approach based on modified Morrow, Smith Watson Topper and Walker equation to find stress and strain amplitude. Finally, generate the results of factor of safety and life expectancy of the steering knuckle of all vehicles. In the design process, basic standards were followed and showed in Figure-4 below.

ARPN Journal of Engineering and Applied Sciences

General Flow chart

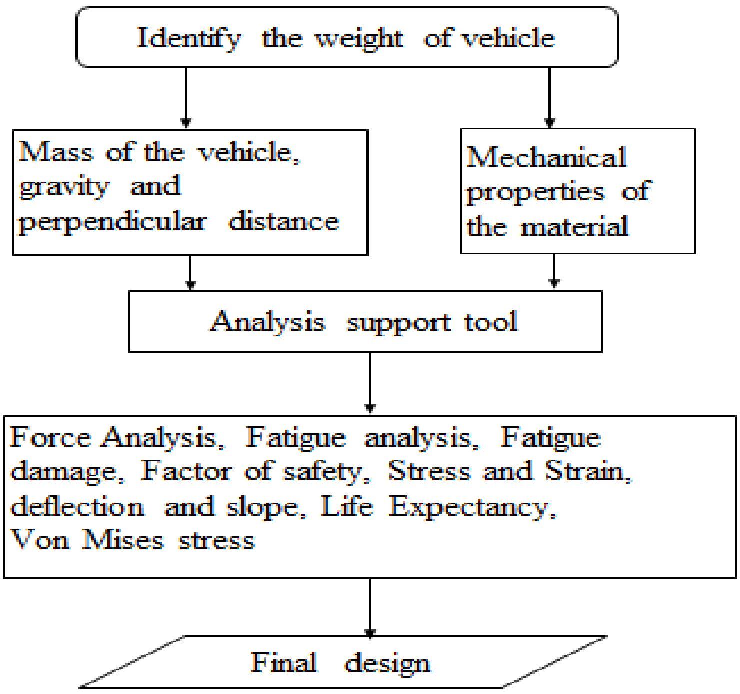

Figure-4. Flow chart Design support tool.

RESULT AND DISCUSSIONS

Description of Analysis Support Tool

The steering knuckle design and analysis support tool for all vehicles was developed via Python and the developed tool can be run on any computer without using the internet connection.

How It Works

To use the developed design support tool, the following steps are required: - first open the tool and feed the appropriate data then click on process. Finally, the result will generate and the first page of the tool is shown in the Table-1 below.

Table-1. Shows the first page of the developed tool.

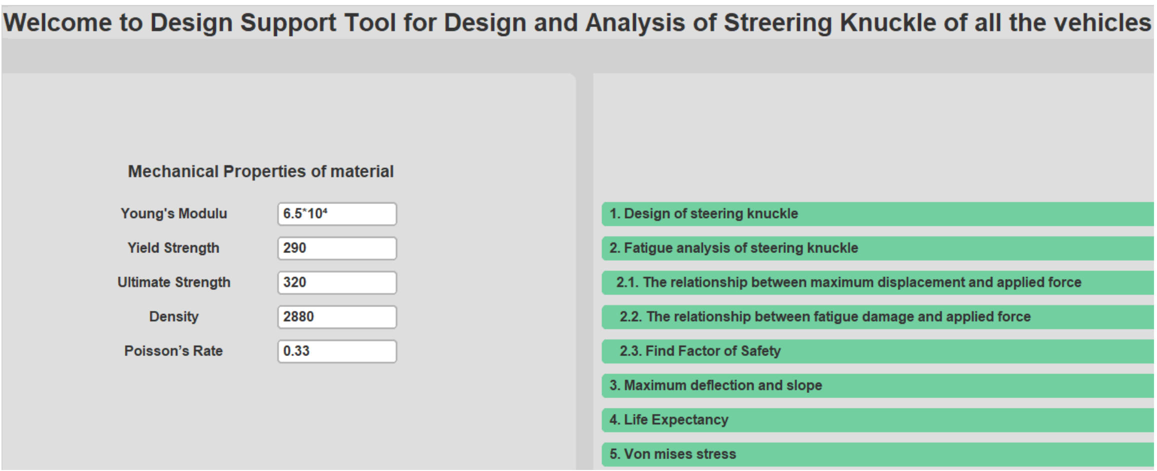

The points that have been done inside the developed tool are as under.

Load Analysis on the Steering Knuckle of the Entire Knuckles

For the determination of forces and moments, required loading situations acting on steering knuckle component which are used inside the tool indicated below and the result is shown in Table-2.

VOL. 18, NO. 12, JUNE 2023 ISSN 1819-6608
ARPN Journal of Engineering and Applied Sciences

$a)\ Braking\ Load = 1.5\ x\ mass\ x\ gravity$

$b)\ Steering\ Load = 45\ to\ 50\ N$

$c)\ Lateral\ Load = 1.5\ x\ mass\ x\ gravity$

$d)\ Moment = Braking\ Load\ x\ perpendicular\ dis\tan ce$

$e)\ Load\ on\ the\ X - axis = 1.5\ x\ mass\ x\ gravity$

$f)\ Load\ on\ the\ Y - axis = 1.5\ x\ mass\ x\ gravity$

$g)\ Load\ on\ the\ Z - axis = 1.5\ x\ mass\ x\ gravity$

$$\text{Re}\,sul\tan t\ Load = \sqrt{F_x^{\ 2} + F_y^{\ 2} + F_z^{\ 2}}$$

Input: Mass of the vehicle, gravity and perpendicular distance

Output: All Forces and Braking moment

Table-2. Shows the result of loading condition on steering knuckle.

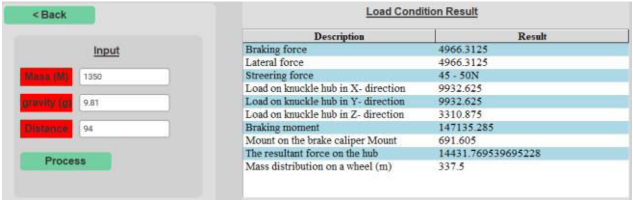

Description	Result
Braking force	4966.3125
Lateral force	4966.3125
Streering force	45 - 50N
Load on knuckle hub in X- direction	9932.625
Load on knuckle hub in Y- direction	9932.625
Load on knuckle hub in Z- direction	3310.875
Braking moment	147135.285
Mount on the brake caliper Mount	691.605
The resultant force on the hub	14431.769539695228
Mass distribution on a wheel (m)	337.5

Fatigue Analysis of Steering Knuckle

The detail stress and strain amplitudes are calculated by using Morrow, SWT and Walker equation to determine the life expectancy is shown in Table-3 and Table-3.1 below.

Input data to the tool

$Modulus\ of\ elasticity\ (E), Fatigue\ strength\ coefficient\ (\sigma'_f), Fatigue\ strength\ exponent\ (b),$

$Fatigue\ ductility\ coefficient\ (\varepsilon'_f), Fatigue\ ductility\ exponent\ (c), (\sigma_a)\ stress\ amplitude,$

$(S_N)\ fully\ reversed\ fatigue\ strength\ at\ the\ desired\ number\ of\ cycles,\ Minimum\ stress\ (\sigma_m),$

$Stress\ Ratio\ (R)\ , Material\ dependent\ exponent\ (\gamma), True\ stress\ at\ fracture\ (\sigma_{ft})$

$(2N_f)\ number\ of\ reversals\ to\ failure\ in\ the\ strain\ life\ test$

Output: Stress & strain amplitude which is used to determine the fatigue life

Table-3. Shows the stress and strain amplitude equation used inside the tool.

Relationship	Stress Life Equation	Strain Life Equation
Morrow	$\sigma_a = S_N.\left(1 - \frac{\sigma_m}{\sigma_{ft}}\right)$	$\varepsilon_a = \frac{\sigma'_f}{E}.\left(1 - \frac{\sigma_m}{\sigma'_f}\right).(2N_f)^b + \sigma'_f.\varepsilon'_f.(2N_f)^{b+c}$
Smith Watson Topper (SWT)	$\sigma_a = S_N.(\frac{2}{1-R})^{-1/2}$	$\varepsilon_a = \frac{\sigma'_f}{E}.[2N_f.(\frac{1-R}{2})^{1/2b}]^b + \varepsilon'_f.[2N_f.(\frac{1-R}{2})^{1/2b}]^c$
Walker	$\sigma_a = S_N(.\frac{2}{1-R})^{-\gamma}$	$\varepsilon_a = \frac{\sigma'_f}{E}.[2N_f.(\frac{1-R}{2})^{1-\gamma/b}]^b + \varepsilon'_f.[2N_f.(\frac{1-R}{2})^{1-\gamma/b}]^c$

VOL. 18, NO. 12, JUNE 2023 ISSN 1819-6608
ARPN Journal of Engineering and Applied Sciences

www.arpnjournals.com

Table-3.1. Result of stress and strain amplitude by Morrow, SWT and Walker equation.

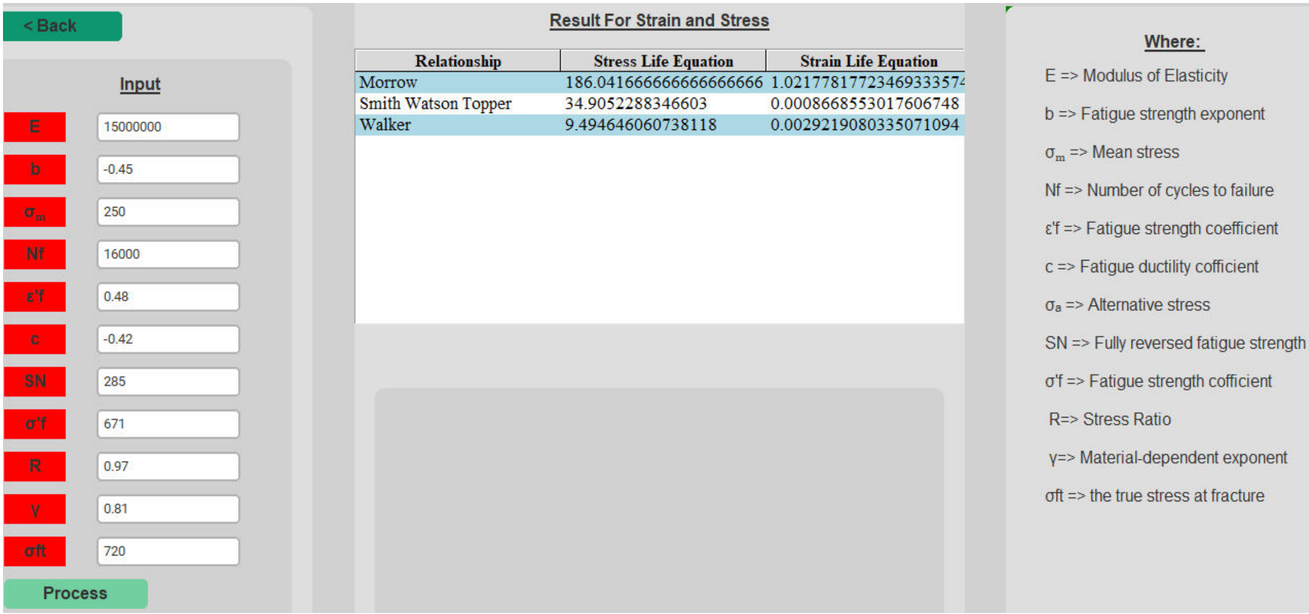

Relationship	Stress Life Equation	Strain Life Equation
Morrow	186.0416666666666666	1.0217781772346933357
Smith Watson Topper	34.9052288346603	0.0008668553017606748
Walker	9.494646060738118	0.0029219080335071094

Displacement vs Each Applied Force

Applying a force causes a displacement, and their connection is more linear than quadratic. This is because exerting forces directly affects how far an object is moved. As force increases, displacement grows. The relationship is linear which is shown in Table-4.

Table-4. The relationship between displacement and applied force.

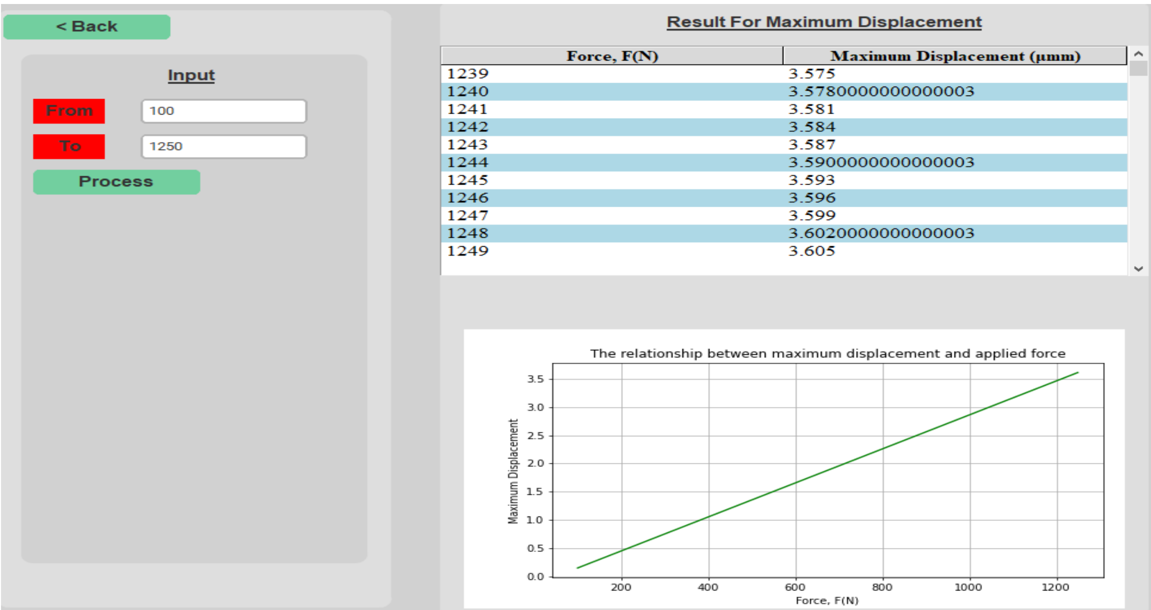

Force, F(N)	Maximum Displacement (μmm)
1239	3.575
1240	3.5780000000000003
1241	3.581
1242	3.584
1243	3.587
1244	3.5900000000000003
1245	3.593
1246	3.596
1247	3.599
1248	3.6020000000000003
1249	3.605

Fatigue Damage vs Each Applied Force

In both constant amplitude loading and variable amplitude loading, fatigue damage rises with applied loading cycles. The linear damage accumulation rule, also called the Palmgren-Miner rule, states that when the damage D reaches unity, the material fails. The relationship between the fatigue damage and applied force is shown in Table-5 below.

VOL. 18, NO. 12, JUNE 2023 ISSN 1819-6608
ARPN Journal of Engineering and Applied Sciences

www.arpnjournals.com

Table-5. The relationship between fatigue damage and applied force.

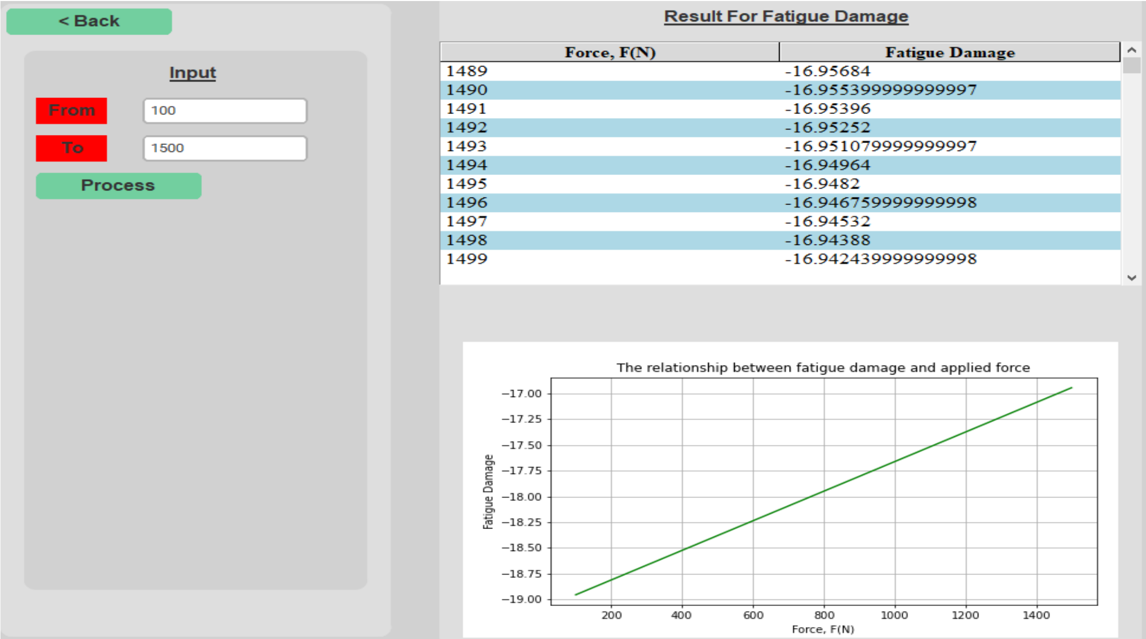

Force, F(N)	Fatigue Damage
1489	-16.95684
1490	-16.955399999999997
1491	-16.95396
1492	-16.95252
1493	-16.951079999999997
1494	-16.94964
1495	-16.9482
1496	-16.946759999999998
1497	-16.94532
1498	-16.94388
1499	-16.942439999999998

Determination of Factor of Safety

The capability of a system's structural capacity to be viable beyond its actual loads is called factor of safety (n) [41]. The result of factor of safety from Soderberg and Goodman equation is shown in Table-6.

a) Soderberg Equation [41].

$$\frac{\sigma_a}{S_e} + \frac{\sigma_m}{S_y} = \frac{1}{n}$$

Where n is the factor of safety

b) Goodman Equation [41].

$$\frac{\sigma_a}{S_e} + \frac{\sigma_m}{S_y} = \frac{1}{n}$$, Where n is the factor of safety

$$S_e = k_a . k_b . k_c . k_a . S_e'$$

Input data

S_e: Endurance limit of a component subjected to reversed bending stress

S_e': Endurance limit stress of a rotating beam subjected to reversed bending stress

K_a : Surface Finish, k_b : Size factor, σ_m : Mean stress

K_d: Modifying factor of stress concentration

σ_y : Yield strength , σ_u : Ultimate strength,

Out Put: Result of Factor of Safety Soderberg and Goodman Equation

Table-6. Shows the result of factor of safety.

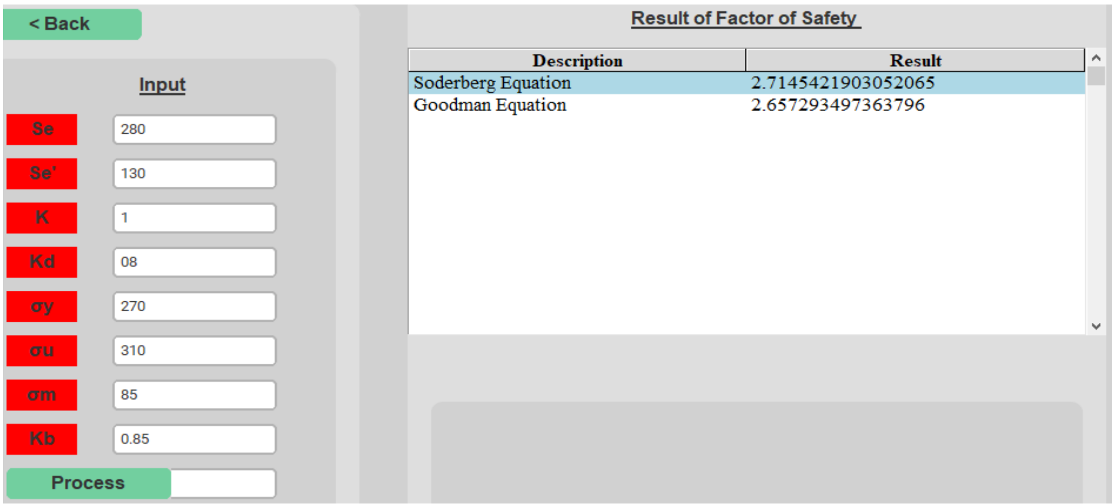

Description	Result
Soderberg Equation	2.7145421903052065
Goodman Equation	2.657293497363796

VOL. 18, NO. 12, JUNE 2023 ISSN 1819-6608
ARPN Journal of Engineering and Applied Sciences

Maximum Deflection and Slope

Deflections are essential to the part's design and analysis. A part's excessive deflection damages the component as well as being visually difficult. It needs remain below the dimensional tolerances of the machined pieces. The slope and deflection are calculated using the basic formula below and the result stated under Table-7. Note that we used the standard SI unit.

$\delta_{max} = \frac{FL^3}{3EI}$ and $\theta = \frac{FL^2}{2EI}$

Where δ_{max} is maximum deflection (m), is slope ($degree$) , L- length (m), E- Modulus of elasticity (N/m2 (m), F-Force (n), F is force (N), and I - Moment of inertia (m4).

Input data: length (L), modulus of elasticity (E), force (F), moment if inertia (I)

Out Put data: Maximum deflection (m) and slope (Radian)

Table-7. The result of Maximum deflection and slope.

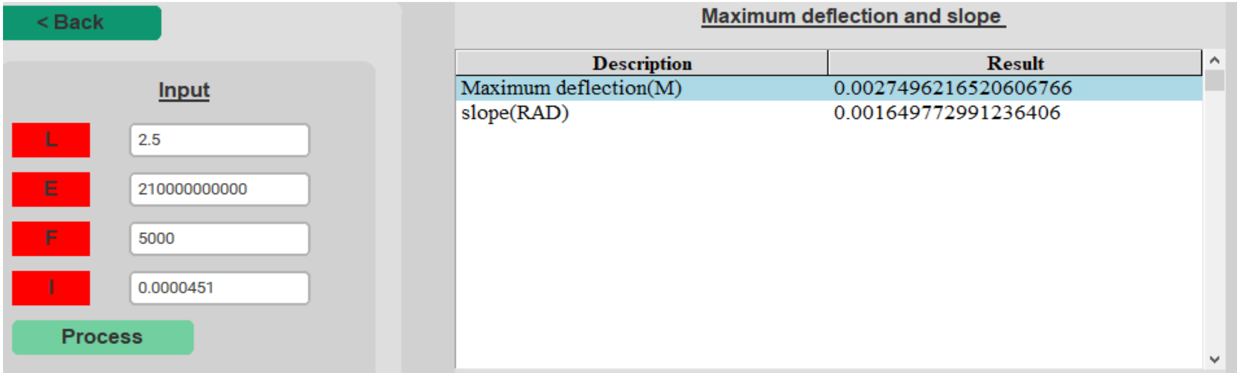

Analysis of Equivalent Stress and Life Expectancy

The equivalent theories are based on the concept of converting a multiaxial stress state to a uniaxial one by finding an equivalent stress and the result is shown in Table-8.

Table-8. The result of Equivalent stress and Life expectancy.

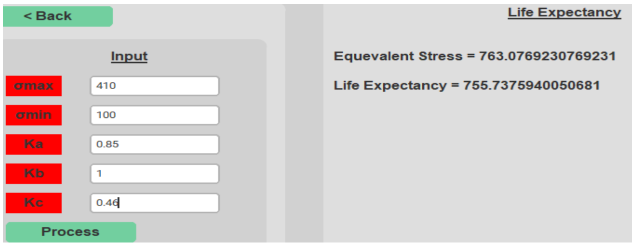

Von Misses Stress

The von Mises stress represents the equivalent stress state of the material before the distortional energy reaches its yielding point and the result can be found by using the Table-9.

Table-9. The result of Von misses stress.

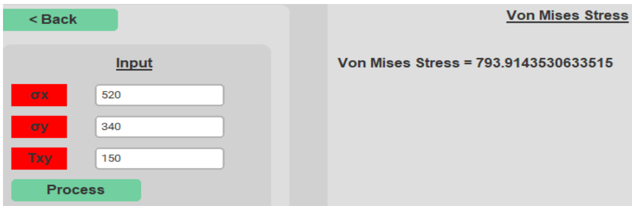

Numerical Sample Load Calculation to Validate the Tool

Assume the total weight of the car is 1350Kg. in order to find the braking load acting on one wheel the total weight of the vehicle must be distribute for four wheels so that the weight of one wheel is 1350/4 = 337.5 kg.

$$a)\ Braking\ Load = 1.5\,x\,337.5\,x\,9.81 = 4966.3125\,kg\,{}^{m}/{}_{s^2}$$

$$b)\ Lateral\ load = 1.5x337.5x9.81 = 4966.3125\,kg\,{}^{m}/{}_{s^2}$$

$$b)\ Moment = Braking\ Load\ x\ perpendicular\ distance$$

$$= 4966.3125\,kg\,{}^{m}/{}_{s^2}\ x94\,mm = 147135.285\,kg\,{}^{m}/{}_{s^2}.mm$$

$$d)\ Load\ on\ the\ X-axis = Load\ on\ the\ Y-axis = 3\,x\,337.5\,x\,9.81 = 9932.625\ kg\,{}^{m}/{}_{s^2}$$

$$e)\ Load\ on\ the\ Z-axis = 1\,x\,mass\ x\ gravity = 3310.875\,kg\,{}^{m}/{}_{s^2}$$

$$\text{Resultant Load} = \sqrt{F_x{}^2 + F_y{}^2 + F_z{}^2} = \sqrt{9932.625^2 + 9932.625^2 + 3310.875^2}$$

$$= 14,431.7695397\,kg\,{}^{m}/{}_{s^2}$$

CONCLUSIONS

The steering knuckle design support tool for all vehicles has been created using Python, and the tool can be used on any computer without an internet connection. The developed tool can calculate the results of all forces acting on the steering knuckle, stress and strain amplitude, stress & strain life approaches by using multiaxial fatigue loading. Additionally, for each applied force, the tool can calculate the maximum displacement produced as well as fatigue damage. Finally, based on the input data, the tool can calculate the factor of safety results using the Goodman and Soderberg equation. The tool can also calculate the steering knuckle's maximum deflection, slope, life expectancy, and equivalent stress. Open source literatures are used to validate the tool. All the developed codes are available with the author.

Data Availability

The data used in this study to support the findings of this research are available from the authors based on request including the developed software.

Conflicts interests

All the authors declare that there is no conflict of interest regarding the publication of this paper.

Statement for Funding

There is no any specific received grant/fund from funding agencies in the public, commercial or not for profit sectors for this research paper.

REFERENCES

[1] F. H. Ad Suhadak, K. A. Zakaria, M. B. Ali, and M. A. Yusuff. 2018. Stress analysis of automobile steering knuckle using finite element method. Int. J. Eng. Technol., 7(3): 28-30, doi: 10.14419/ijet.v7i3.17.16617.

[2] S. Karri, D. Lohith Varma, N. Patchipala and S. Jajimoggalaa. 2021. CAE Analysis on weight optimization in steering knuckle using aluminium alloy. Turkish journal of computer and mathematics.

[3] T.-F. Zach and M.-C. Dudescu. 2021. The Topological Optimization and the Design for Additive Manufacturing of a Steering Knuckle for Formula SAE Electric Vehicle. MATEC Web Conf., 343: 04011, doi: 10.1051/matecconf/202134304011.

[4] S. Srivastava, S. Salunkhe, S. Pande, and B. Kapadiya. 2020. Topology optimization of steering knuckles structure. Multidisc. Des. Optim. 11, 4.

[5] C. P and K. R. 2020. Weight Optimization of Hub and Knuckle Using Topology Optimization. Int. J. Mech. Eng., 7(6): 20-23, doi: 10.14445/23488360/ijme-v7i6p103.

[6] D. Pujari and R. N. Yerrawar. 2018. Design And Experimental Evaluation of Steering Knuckle Arm For Stiffness. Journal of Mechanical and Civil Engineering, 15(4): 34-43, doi: 10.9790/1684-1504053443.

[7] G. A. Prabhu, K. Muninathan, O. L. Kanna, G. Monish, and S. R. Arun. 2020. Static Analysis of Aluminum 6063 Alloy for Steering Knuckle Application in Student Formula Car. IOP Conf. Ser. Mater. Sci. Eng., 923(1) doi: 10.1088/1757-899X/923/1/012007.

[8] L. Rajesh Kumar, S. Sivalingam, K. Prashanth and K. Rajkumar. 2020. Design, analysis and optimization of steering knuckle for all terrain vehicles. AIP Conf. Proc., 2207(February), doi: 10.1063/5.0000044.

[9] Zhang Derong. 2019. Failure Analysis and the Optimization for the Static Pull Test of Steering Knuckle. Mech. Eng. Technol. 08(02): 80-86.

[10] K. Loganathan and M. Akash. 2018. Design and Analysis of Steering knuckle component for Terrain vehicle. Int. J. Recent Trends Eng. Res. 4(3): 36-42.

[11] Yu Z. Y., Zhu S.P., Liu Q. and Liu Y. 2017. A new energy-critical plane damage parameter for multiaxial fatigue life prediction of turbine blades. Materials. 10(5): 513.

[12] Zhu S. P., Liu, Q., Peng, W. and Zhang, X.C. 2018. Computational-experimental approaches for fatigue reliability assessment of turbine bladed disks. International Journal of Mechanical Sciences. 142: 502-517.

[13] Liao D., Zhu S.P. and Qian G. 2019. Multiaxial fatigue analysis of notched components using combined critical plane and critical distance approach. International Journal of Mechanical Sciences. 160: 38-50.

[14] Liao D., Zhu S. P., Keshtegar, B., Qian, G. and Wang, Q. 2020. Probabilistic framework for fatigue life assessment of notched components under size effects. International Journal of Mechanical Sciences. 181: 105685.

[15] Dantas R., Correia J. A., Lesiuk G., Rozumek D., Zhu, S. P., De Jesus, A., Susmel, L. and Berto, F. 2021. Evaluation of multiaxial high-cycle fatigue criteria under proportional loading for S355 steel. Engineering Failure Analysis. 120: 105037.

[16] Correia J. A., Carvalho H., Lesiuk G., Mour~ao A., Grilo L.F., de Jesus A. and Calçada R. 2020. Fatigue crack growth modelling of F~ao Bridge puddle iron under variable amplitude loading. International Journal of Fatigue. 136: 105588.

[17] He J. C., Zhu S. P., Liao D. and Niu X. P. 2020. Probabilistic fatigue assessment of notched components under size effect using critical distance theory. Engineering Fracture Mechanics. 235: 107150.

[18] Viana C. O., Carvalho H., Correia J. A., Montenegro P. A., Heleno, R. P., Alencar, G. S., De Jesus, A. M. and Calçada, R. 2021. Fatigue assessment based on hot-spot stresses obtained from the global dynamic analysis and local static sub-model. International Journal of Structural Integrity. 12(1): 31-47.

[19] Mi J., Li Y. F., Peng W., Huang H. Z. 2018. Reliability analysis of complex multi-state system with common cause failure based on evidential networks. Reliab. Eng. Syst. Saf. 174, 71-81.

[20] Mi J., Li Y. F., Yang Y. J., Peng W., Huang H.Z. 2016. Reliability assessment of complex electromechanical systems under epistemic uncertainty. Reliab. Eng. Syst. Saf. 152, 1-15.

[21] Jørgensen J. B., Sørensen B. F., Kildegaard C. 2018. Tunneling cracks in full scale wind turbine blade joints. Eng. Fract. Mech. 189, 361-376.

[22] Maktouf W., Ammar K., Naceur I. B., Saï K. 2016. Multiaxial high-cycle fatigue criteria and life prediction: Application to gas turbine blade. Int. J. Fatigue. 92, 25-35.

[23] Žužek B., Burja J. 2017. Investigation of nickel alloy fan blade failure in a flue gas desulfurization unit. Eng. Fail. Anal. 82, 855-861.

[24] Li H., Huang H. Z., Li Y. F., Zhou J., Mi J. 2018. Physics of failure-based reliability prediction of turbine blades using multi-source information fusion. Appl. Soft Comput. 72, 624-635.

[25] Gao J., An Z., Kou H. 2018. Fatigue life prediction of wind turbine rotor blade composites considering the combined effects of stress amplitude and mean stress. Proc. Inst. Mech. Eng. O J. Ris. Reliab.

[26] Li X.Y., Li Y.F., Huang H.Z., Zio E. 2018. Reliability assessment of phased-mission systems under random shocks. Reliab. Eng. Syst. Saf. 180, 352-361.

[27] Shinde V., Jha J., Tewari A. and Miashra S. 2018. Modified rainflow counting algorithm for fatigue life calculation. Proceedings of Fatigue, Durability and Fracture Mechanics. p. 381.

[28] Park J. and Nelson D. 2000. Evaluation of an energy-based approach and a critical plane approach for predicting constant amplitude multiaxial fatigue life. International Journal of Fatigue. 22(1): 23-29.

[29] Rovinelli A., Messner M. C. and Sham T.L. 2021. A comprehensive comparison between different multiaxial cycle counting procedure. Pressure Vessels and Piping Conference. p. 38.

[30] Samavatian V., Iman-Eini H. and Avenas Y. 2018. An efficient online time-temperature-dependent creep-fatigue rainflow counting algorithm. International Journal of Fatigue. 116: 284-292.

[31] Sarkar S., Kumar C.S. and Nath A.K. 2019. Investigation on the mode of failures and fatigue life of laser-based powder bed fusion produced stainless steel parts under variable amplitude loading conditions. Additive Manufacturing. 25: 71-83.

[32] Scalet G. 2021. A convex hull-based approach for multiaxial high-cycle fatigue criteria. Fatigue and Fracture of Engineering Materials and Structures. 44(1): 14-27.

[33] Schubnell J., Hardenacke V. and Farajian M. 2017. Strain-based critical plane approach to predict the fatigue life of high frequency mechanical impact (HFMI)-treated welded joints depending on the material condition. Welding in the World. 61(6): 1199-1210.

[34] Shang D. G. and Wang D. J. 1998. A new multiaxial fatigue damage model based on the critical plane approach. International Journal of Fatigue. 20(3): 241-245.

[35] Skibicki D., Lipski A. and Pejkowski. 2018. Evaluation of plastic strain work and multiaxial fatigue life in CuZn37 alloy by means of thermography method and energy-based approaches of Ellyin and Garud. Fatigue and Fracture of Engineering Materials and Structures. 41(12): 2541-2556.

[36] Socie D. 1987. Multiaxial fatigue damage models. Journal of Engineering Materials and Technology. 109(4): 292-298.

[37] Topper T. H. and Lam T. S. 1997. Effective strain-fatigue life data for variable amplitude fatigue. International Journal of Fatigue. 19: 137-143.

[38] Smith K. N., Watson P. and Topper T. H. 1970. A Stress- strain function for the fatigue of metals. Journal of Materials. 5(4): 767-778.

[39] Suhir E., Ghaffarian R. and Yi S. 2017. Probabilistic Palmgren–Miner rule, with application to solder materials experiencing elastic deformations. Journal of Materials Science: Materials in Electronics. 28(3): 2680-2685.

[40] Wang Y. and Susmel L. 2016. The Modified Manson-Coffin Curve Method to estimate fatigue lifetime under complex constant and variable amplitude multiaxial fatigue loading. International Journal of Fatigue. 83: 135-149.

[41] R. S. Khurmi and J.K. Gupta. 2005. A text book of Machine Design. Eurasia publishing house (PVT) LTD.110055.

[42] Y. Jiang *et al*. 2007. An experimental evaluation of three critical plane multiaxial fatigue criteria Int J Fatigue.

[43] D. G. Shang *et al*. Creep-fatigue life prediction under fully-reversed multiaxial loading at high temperatures Int J Fatigue (2007)

[44] G. Q. Sun *et al*. 2010. Prediction of fatigue lifetime under multiaxial cyclic loading using finite element analysis Mater Des.

[45] N. Jayaraman *et al*. 11989. Torsional and biaxial (tensions-torsion) fatigue damage mechanisms in Waspaloy at room temperature Int J Fatigue.

[46] B. F. Zhao *et al.* 2021. A new multiaxial fatigue life prediction model for aircraft aluminum alloy Int J Fatigue.

[47] Carpinteri A., Spagnoli, A. and Vantadori S. 2011. Multiaxial fatigue assessment using a simplified critical plane-based criterion. International Journal of Fatigue. 33(8): 969-976.

[48] Araujo J.A., Carpinteri A., Ronchei C., Spagnoli A. and Vantadori S. 2014. An alternative definition of the shear stress amplitude based on the Maximum Rectangular Hull method and application to the C-S (Carpinteri-Spagnoli) criterion. Fatigue and Fracture of Engineering Materials and Structures. 37(7): 764-771.

[49] Carpinteri A., Berto F., Campagnolo A., Fortese G., Ronchei C., Scorza D. and Vantadori S. 2016. Fatigue assessment of notched specimens by means of a critical plane-based criterion and energy concepts. Theoretical and Applied Fracture Mechanics. 84: 57-63.

[50] Bohme SA, Vinogradov A., Papuga J., Berto F. 2021. A novel predictive model for multiaxial fatigue in carburized bevel gears. Fatigue Fract Eng Mater Struct. 44: 2033- 2053.

[51] Frendo F, Marulo G, Chiocca A, Bertini L. 2020. Fatigue life assessment of welded joints under sequences of bending and torsion loading blocks of different lengths. Fatigue Fract Eng Mater Struct. 43: 1290- 1304.

[52] Fatemi A. and Socie D. F. 1988. A critical plane approach to multiaxial fatigue damage including out-of-phase loading. Fatigue and Fracture of Engineering Materials and Structures. 11(3): 149-165.

[53] Jordan E. H., Brown M. W. and Miller K. J. 1985. Fatigue under severe nonproportional loading. ASTM Special Technical Publication. pp. 569-585.

[54] Smith, K. N., Watson P. and Topper T. H. 1970. A Stress- strain functions for the fatigue of metals. Journal of Materials. 5(4): 767-778.

[55] Qing-Yun Deng, Shun-Peng Zhu, Jin-Chao He, Xue-Kang Li, Andrea Carpinteri. 2022. Multiaxial fatigue under variable amplitude loadings: review and solutions. International Journal of Structural Integrity.